Electronic Supplementary Material (ESI) for Materials Chemistry Frontiers.

Supporting Information

Concisely Modularized Assembling of Graphene-Based Thin Films with Promising Electrode Performance

Weiwei Wei[a], Rohit L. Vekariy[a], Chuanting You[b], Yafei He[a], Ping Liu[a], Dongqing Wu[a]*, Fan Zhang[a]*

[a] School of chemistry and chemical Engineering, Shanghai JiaoTong University, Dongchuan Road 800, 200240, Shanghai, P.R. China.
[b] College of Materials Science and Engineering, Fujian Agriculture and Forestry University, P. R. China

Table of Content

1 Experimental section:

Materials

Cellulose nanofiber (CNF) and flake graphite were purchased from Kaixiang New Materials Shanghai Co., Ltd. 1-ethyl-3-methylimidazolium tetrafluoroborate ($EMIBF_4$) was achieved from Aladdin Chem. Co., Ltd. (China). All chemical reagents were analytical grade and directly used without further treatment. The battery case for supercapacitor was made by Kuangxun Electronics Co., Ltd. (Shanghai, China). All materials were commercially available and employed without further purification. A poly (tetrafluoride ethylene) (PTFE) membrane (74mm in diameter, 0.22um pore size) was got from

Preparation of CNF/RGO composite film

Graphene oxide (GO) was synthesized via typical Hummers method, and then reduced by hydrazine hydrate to obtain reduced graphene oxide (RGO). In a typical procedure, to a solution of CNF (210.0 mg, 1wt% in 10 mL of deionized water) was slowly added the freshly prepared RGO powder (12.0 mg). Afterwards, this CNF/RGO slurry was fully stirred for 10 min., and then ultrasonically vibricated under 60~80 ^oC for 2 hours. Such performance was repeated for at least 5 times. A homogenous solution was formed. Subsequently, upon the vacuum assistance, the resulting solution of RGO/CNF was slowly filtrated through a poly (tetrafluoride ethylene) (PTFE) membrane (74-mm diameter, 0.22-um pore size) to form an ultrathin hydrogen gel film on the filter. Furthermore, the film was naturally dried under ambient conditions for more than one day. The thin-film sample (donated as CNF-RGO-85) was peeled readily from the polymer filter. By changing the ratio of RGO/CNF in 65/35, 75/25 or 90/10 wt%, a series of GRO/CNF composite thin films termed as CNF-RGO-65, 70, 90, respectively, were fabricated under the same performance.

Preparation of GO/CNF composite film and its post-reduced sample

GO (12 mg) and CNF (CNF (210 mg, 1wt% in 10 mL of deionized water) in a ratio of

85:15 wt% were employed in water (10mL) to form a homogenous solution upon fully stirred for 10 min., and then ultrasonically vibricated under 60~80 ^oC for 2 hours. Subsequently, upon the vacuum assistance, the resulting solution of GO/CNF was slowly filtrated through a poly (tetrafluoride ethylene) (PTFE) membrane (74-mm diameter, 0.22-um pore size) to form an ultrathin hydrogen gel film on the filter. After dried under ambient conditions, a free standing GO/CNF film was peeled from the polymer filter. Upon dipped in hydroiodic acid for a reduction treatment of 48h, and then washed with water, dried under ambient conditions for more than one day, the reduced RGO/CNF film termed as **Red-GO-CNF-85** was achieved.

Preparation of multi-layer electrode

The multi-layer electrodes were manipulated by layer-by-layer stacking the 10-μm-thickness thin film of **RGO-CNF-85** and commercial ionic liquid ($EMIBF_4$) as electrolyte. In a general fabrication, at first, ionic liquid was uniformly dipped on the battery case to fix the first layer of **RGO-CNF-85**, and then ionic liquid was coated on the surface of this layer to get a one-layered electrode. Another layer was stacked continuously on the top of this one-layered electrode, and then coated with ionic liquid, to achieve a two-layered electrode. The same process was repeated to fabricate a series of multi-layered electrodes with three, five, seven and ten layers of **RGO-CNF-85** (donated as **3, 5, 7, 10L-RGO-CNF-85**, respectively), the two symmetric multi-layered electrodes were separated with cellulose acetate membrane and compressed into button cell case. All of the operation was carried in glovebox.

Characterization methods

Fourier transform infrared spec-transcopy (FT-IR) spectra were recorded on a Bomen MB154 spectrometer with KBr pellets. Thermo-gravimetric analysis was carried out in a Mettler-Toledo TGA/SDTA852 thermal analysis in a dynamic atmosphere of nitrogen (flow rate = 30 cm^3min^{-1}). The samples for tensile test were tailored into strip with the width of 3 mm and length of 15 mm by a bistoury. The testing was carried out via Instron 3342 universal testing machine (Instron, USA) under 25 ^oC.

Raman spectra were recorded on a RM2000 microscopic confocal Raman spectrometer employing a h14 nm laser beam. X-ray diffraction (XRD) analyses were performed on a Bruker D8 Advance diffractometer with Cu kradiation (≈ 1.54˚A) at 40 kV and 30 mA. Morphological were observed on an Atomic Force Microscope (AFM) at air atmosphere and field emission gun scanning electron microscopy (FE-SEM, Hitachi S4800) at an accelerating voltage of 15kV.

Electrochemical measurement

Cyclic voltammetry analysis was carried out on a CHI660D electrochemical workstation (Shanghai, China) with a two-electrode supercapacitor setup. In our experiment, 1-ethyl-3-methylimidazolium tetrafluoroborate (EMIBF$_4$) as electrolyte, acetyl cellulose based paper was utilized as dissepiment to separate two electrodes. Cyclic voltammetry was performed in the voltage range of 0 to 4 V at different scan rates ranging from 10 to 100 mV s^{-1}. Galvanostatic charge–discharge experiment was carried out in potential range from 0 to 4 V with applied current density increased gradually from 0.2 to 1A/g. The electrochemical impedance spectroscopy (EIS) analysis was operated under the condition: AC voltage amplitude 5 mV s^{-1}, frequency range: $1 \times 10^5 \sim 1 \times 10^{-2}$ Hz at 0.5 V. The conductivity testing was carried out on an RTS-1345 four-electrode system. Conductance was tested though four probe method. The specific galvanostatic capacitance (C_g) was calculated by Equation 1, specific volumteric capacitance (C_v) was calculated by Equation 2 and the area capacitance (C_{area}) was calculated by Equation 3.

C_g (F g^{-1}) = $I\,dt/\,mV$ (1)

C_v(F cm^{-3})= $\rho \times C_g$ (2)

where I is the constant discharge current (Ag^{-1}), dt is the discharge time (s), V is the discharge potential(V), ρ is the density of electrode (g cm^{-3}), m is the quality.

The volumetric energy density of electrode (E).

E(Wh L^{-1}) = $0.5\ CvU^2/\ 3.6$ (3)

The power density of electrode (P) was calculated via equation (4)

P (W L^{-1})= $3600 \times E\ /\ dt$ (4)

Where dt is discharge time.

2. Experiment data

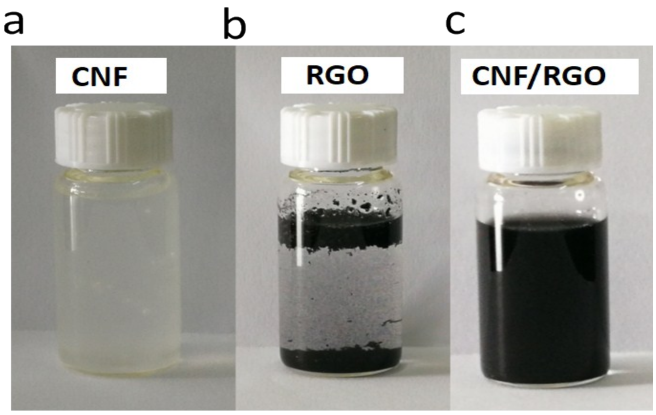

Figure S1. Digital images of (a) CNF dispersion (b) RGO dispersion (c) RGO/CNF dispersion with 85 w% RGO in water.

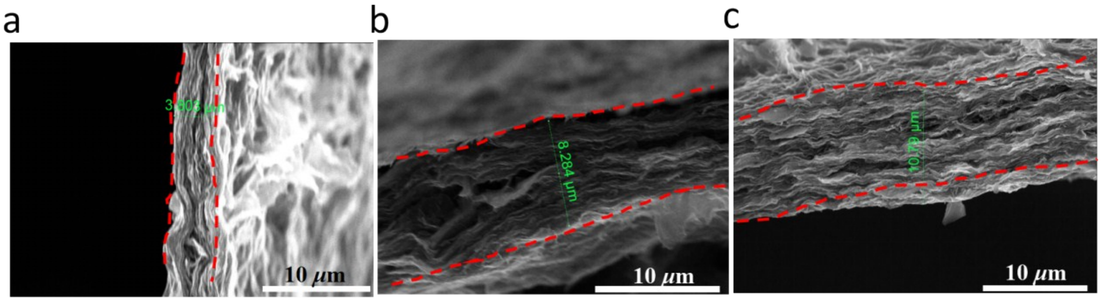

Figure S2. Side view sof SEM images of the different **CNF-RGO-85** samples with the different thickness (a) ~ 4 μm, (b) ~ 8 μm (c) ~ 10 μm, respectively.

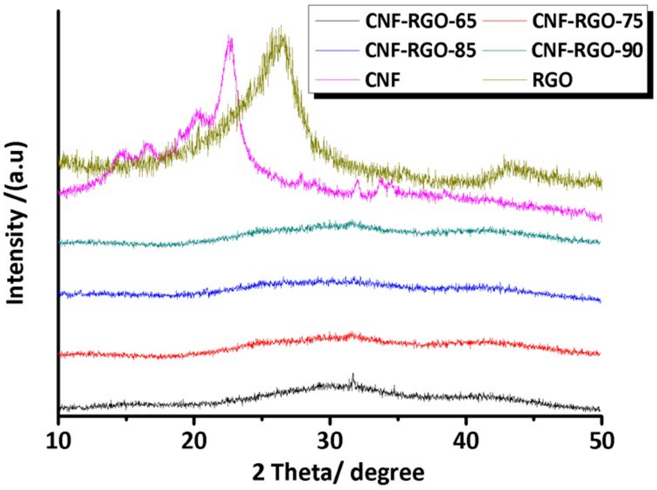

Figure S3. The XRD patterns of **CNF-RGO-*n* (n: 65, 75, 85, 90)** samples

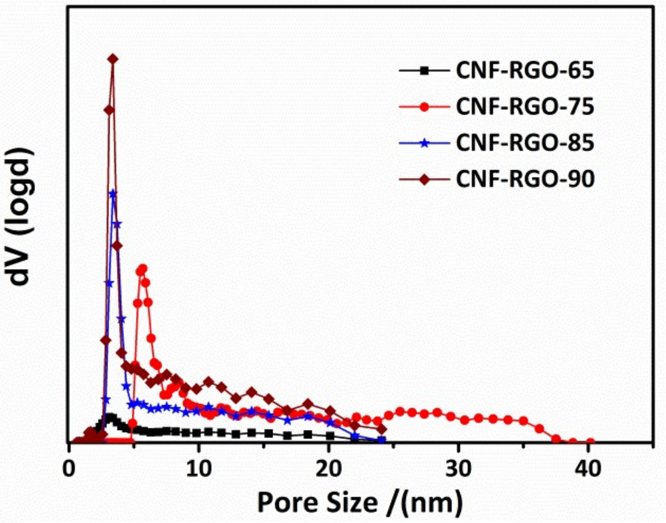

Figure S4. The pore size distributions of **CNF-RGO-*n* (*n*: 65, 75, 85, 90)**

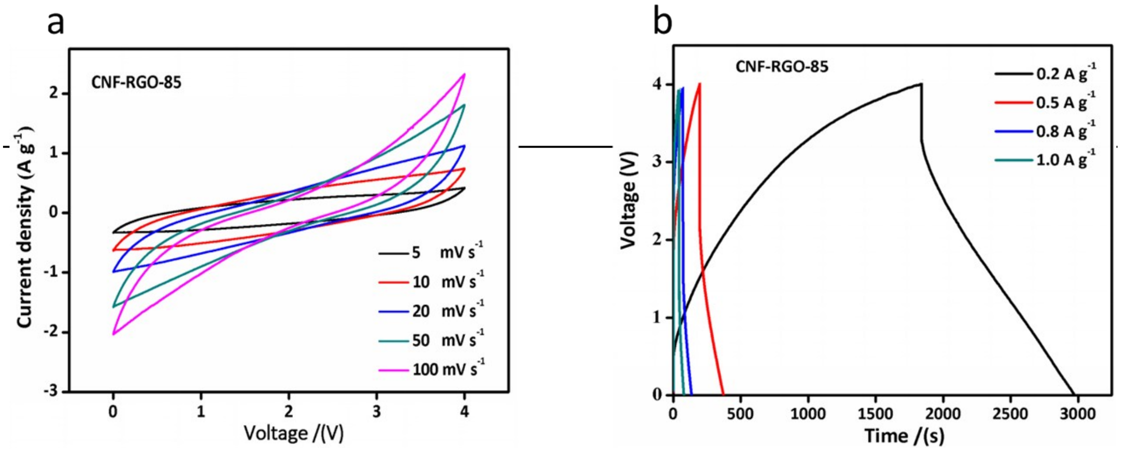

Figure S5. The operation voltage investigation for single electrode of **CNF-RGO-85** (a) CV curve of device working under different voltage window (b) GCD curve of device

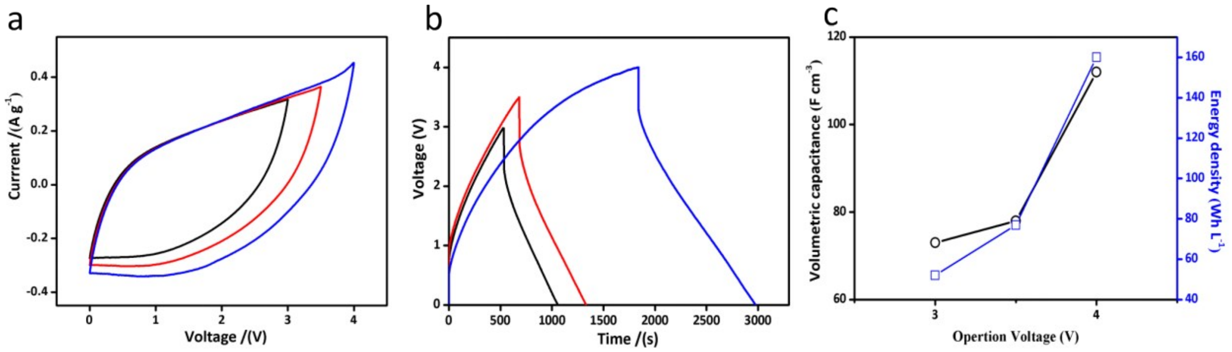

Figure S6. (a) The CV curves of **single CNF-RGO-85** at the scan rate from 5 mV s^{-1} to100 mV s^{-1}; (b) the GCD curves of **single CNF-RGO-85**, the IR drop is 0.75 V, 0.83 V, ,1.7 V at 0.2 A g^{-1}, 0.5 A g^{-1}, 0.8 A g^{-1}, 1.0 A g^{-1}

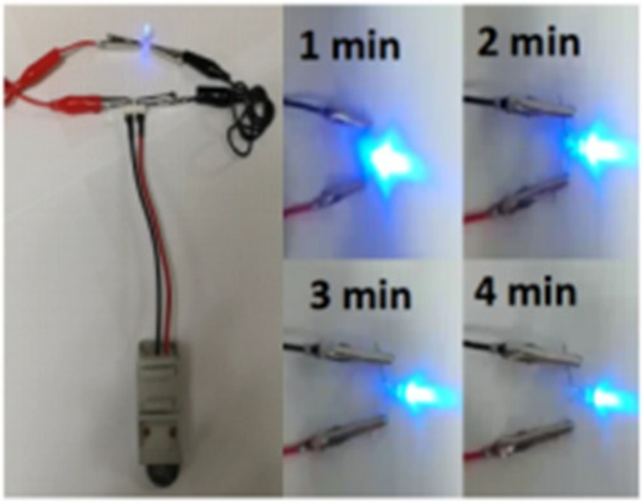

Figure S7. Digital photos of blue LED that is lightened by tandem device.

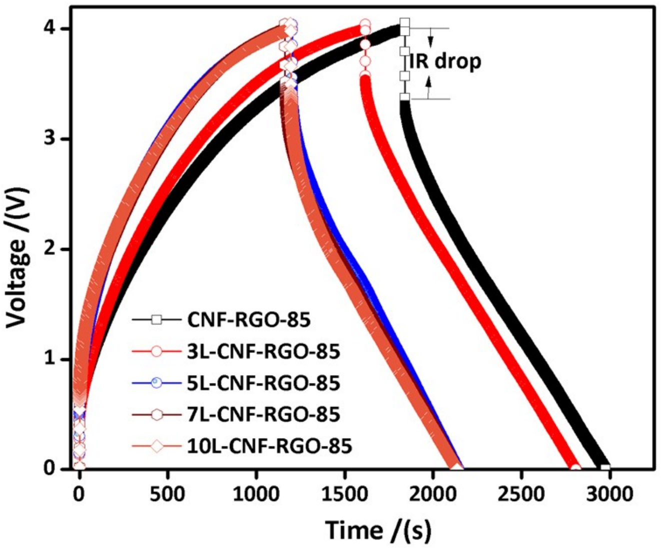

Figure S8. The Galvanostatic charge/ discharge profiles of single **CNF-RGO-85, 3L-CNF-RGO-85, 5L-CNF-RGO-85, 7L-CNF-RGO-85 and 10L-CNF-RGO-85** at a current density of 0.32 A cm^{-3}.

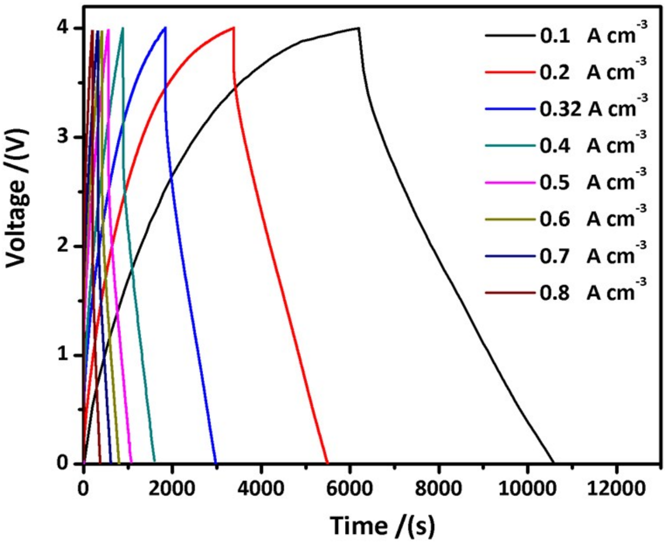

Figure S9. The GCD curve of single CNF-RGO-85 at different volumetric current density

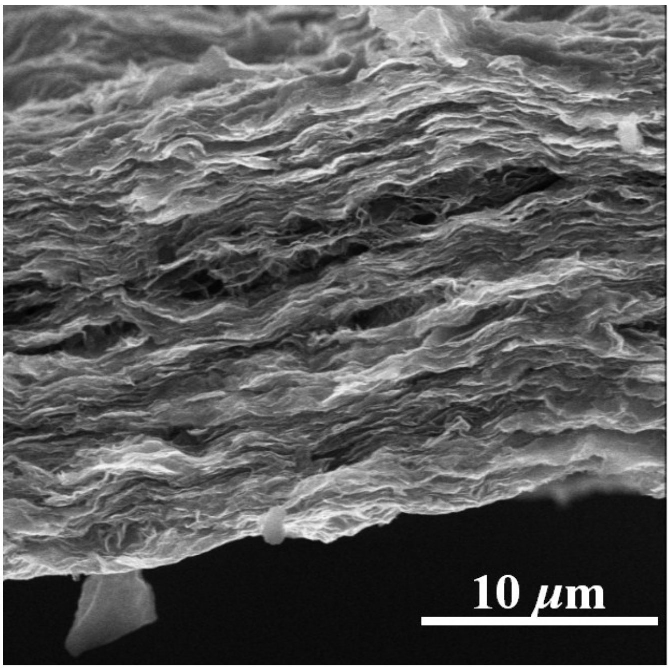

Figure S10. The SEM images of cross-section of signal or 3L-CNF-RGO-85 electrode after 2000 charge-discharge cycles.

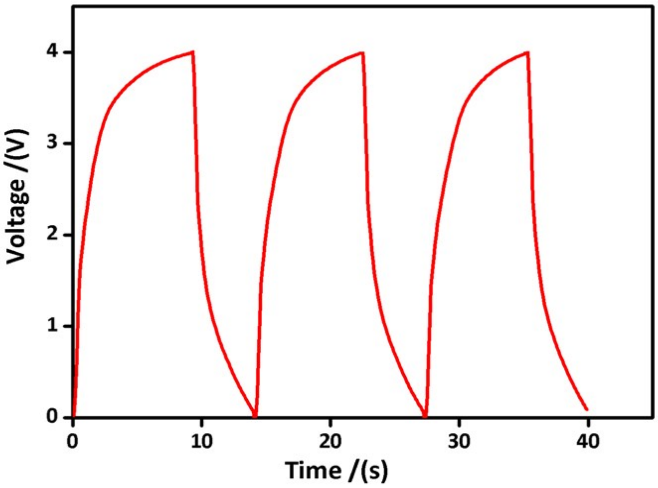

Figure S11. The GCD curve of **Red-RGO-CNF-85** at 0.2 A g^{-1}. The GCD curve exhibited that the electrode cannot store electron during charge-discharge process.

Table S1. The electrochemical performance of multi-layered electrodes

Samples	Layers	Volumetric capacitance (F cm^{-3} at 0.32 A cm^{-3})	Energy density (Wh L^{-1})	Power density (W L^{-1})
CNF-RGO-85	1	115	160	511
3L-CNF-RGO-85	3	112	180	545
5L-CNF-RGO-85	5	101	136	518
7L-CNF-RGO-85	7	96	122	440
10L-CNF-RGO-85	10	100	140	539

Table S2. Comparison of electrochemical performance between the **CNF-RGO-*n*** thin films and other high volumetric energy density electrodes.

Electrodes	electrolyte	Voltage Windows (V)	Volumetric energy density (Wh L^{-1})	Volumetric power density (W L^{-1})	Reference
CNF-RGO-*n*	Ionic liquid	0~4	122-180	440-545	This work
VNNDs@CNSs	KOH/PVA	0-0.9	30-14	240-64500	1
$NiCo_2O_4$/NGN/CNTs//NGN@CNTs	KOH aqueous	0-1.5	25.90	9389	2
AC3.2-SC	KOH/PVA	0-1	0.89	209	3
MX@rHGO	3M H_2SO_4 aqueous	-0.7-0.3	38.6	206	4
PAGH	1M H_2SO_4 aqueous	0-1	7.98	25	5
Graphene	H_2SO_4/PVA	0-1	370	416000	6
RGO@CNT	Ionic liquide	0-4	117.2	424000	7
AC//C@$Li_4Ti_5O_{12}$	$LiPF_6$	1.5-2.5	57	2600	8
Carbon fiber	PVA/H3PO4	0-1	6.3	1085	9
Compressed a-MEGO	$TEABF_4$ /AN	0-3.5	48	----	10

Reference:

1. Q. W. Li, Y. Chen, J. B. Zhang, K. F. Huo, *Nano Energy*, 2018, **51**, 128-136
2. S. H. Yue, H. Tong, L. Lu, W. W. Tang, W. L. Bai, F. Q. Jin, Q. W. Han, J. P. He, J. Liu, X. G. Zhang, *J. Mater. Chem. A*, 2017, **5**, 689–698.
3. J. Z. Chen, K. L. Fang, Q. Y. Chen, C. P. Wong, *Nano Energy*, 2018, **53**, 337-344
4. Z. M. Fan, Y. S. Wang, Z. M. Xie, Y. Y. Liu, *Adv. Sci.*, 2018, **5**, 1800750
5. Z. Q. Song, W. Y. Li, Y. Bao, L. Niu, *Carbon*, 2018, **136**, 465348
6. A. Chaichi, Y. Wang, M. R. Gartia, *ACS. Appl. Mater. Interfaces*, 2018, **10**, 21235-21245
7. P. Duy Tho, T. H. Lee, D. H. Luong, F. Yao, A. Ghosh, L. Viet Thong, T. H. Kim, B. Li, J. Chang and Y. H. Lee, *ACS Nano*, 2015, **9**, 2018-2027
8. H. G. Jung, N. Venugopal, B. Scrosati and Y. K. Sun, *J. Power Sources*, 2013, **221**, 266-271.
9. N. Jung, S. Kwon, D. Lee, D. M. Yoon, Y. M. Park, A. Benayad, J. Y. Choi and J. S. Park, *Adv. Mate.*, 2013, **25**, 6854-6858
10. S. Murali, N. Quarles, L. L. Zhang, J. R. Potts, Z. Tan, Y. Lu, Y. Zhu and R. S. Ruoff, *Nano Energy*, 2013, **2**, 764-768.